Revista Brasileira de Farmacognosia 28 (2018) 474–480

Brazilian Journal of Pharmacognosy
REVISTA BRASILEIRA DE FARMACOGNOSIA
www.elsevier.com/locate/bjp

Original Article

^{1}H NMR-based nontargeted metabonomics study of plasma and urinary biochemical changes in Kudouzi treated rats

Jie Chen[a,1], Chenxu Zhang[a,1], Xiuli Wu[a,c,d], Hongyan Ji[b], Wei Ma[a], Shijie Wei[b], Liming Zhang[a,c,d,*], Jing Chen[a,c,d,*]

[a] School of Pharmacy, Ningxia Medical University, Yinchuan, China
[b] Institute of Clinical Pharmacology, General Hospital of Ningxia Medical University, Yinchuan, China
[c] Ningxia Engineering and Technology Research Center for Modernization of Hui Medicine, Yinchuan, China
[d] Key Laboratory of Hui Ethnic Medicine Modernization, Ministry of Education (Ningxia Medical University), Yinchuan, China

ARTICLE INFO

Article history:
Received 6 January 2018
Accepted 25 May 2018
Available online 15 June 2018

Keywords:
^{1}H NMR
Metabonomic
Oral subacute toxicity
Kudouzi
Biochemistry analysis

ABSTRACT

Kudouzi (*Sophora alopecuroides* L., Fabaceae) is an effective folk medicine, but it always causes a hepatic and renal toxicity in clinical therapy. The toxic mechanism remains unclear. This paper detected the urinary and plasma metabolites alteration by ^{1}H NMR-based metabonomics study in Kudouzi-induced rats to evaluate the toxic mechanism for clinical security. The male Sprague-Dawley rats were orally dosed with 0.5 and 1 g Kudouzi/kg weight once per day for consecutive 14 days. Urine samples were collected at day −1 (before treatment), and days 7, 14, and 21 for NMR analysis, respectively. Plasma samples were harvested at day 14 for NMR and biochemical analysis. The metabonomic profiling of Kudouzi-treated rats differed from that of the vehicle. This was confirmed by the biochemistry analysis. The accumulated subacute toxicity of Kudouzi was visible with dosing time, and persisted at day 21 even after the disposal was ended. The observable biochemical pathways alterations included inhibited TCA cycle, activated anaerobic glycolysis, perturbed amino acids metabolism, and disordered gut microbiota. The results evidenced the toxicity mechanism of Kudouzi from a systematic and holistic view.

Introduction

Chinese medicine 'Kudouzi' (*Sophora alopecuroides* L., Fabaceae) is a plant in the genus *Sophora*. It is bitter in taste, cold in nature, and possesses various clinical effects such as heat clearing, detoxifying, analgesic, insecticidal, anti-bacterial, and anti-inflammation (Yang and Yu, 1998; Ren, 2000). Hence it has been clinically used to treat the fever, inflammation, edema and pain (Xiao, 1993). However, *S. alopecuroides* has an extremely strong clinical toxicity; hitherto, the underlying toxic mechanism and potential biomarkers have not yet been recognized, which seriously restricted its clinical application.

Metabonomics is widely used as a powerful tool to investigate the toxicity of Traditional Chinese Medicines (TCM) by tracing the metabolic profiles of biofluids, tissues, and cells, which contain a mixture of metabolites. The abnormal variations of biomolecules in biofluids induced by drugs are rewarding to intensively understand the disease or toxic mechanism (Boudonck et al., 2009a,b). It has been successfully applied to evaluate the toxicity of TCM such as *Aconite lateralis* (Cai et al., 2013), *Pinellia ternate* (Zhang et al., 2013), and *Ricinus communis* (Guo et al., 2014) or some xenobiotics like benalaxyl (Wang et al., 2018), maleic acid (Wu et al., 2017), arsenic (Yin et al., 2017), and 3-MCPD (Ji et al., 2016). Moreover, the obtained results suggested that, for a toxicity evaluation, metabonomics analysis is much more sensitive than traditional toxicological methods (Wang et al., 2018).

Mass spectrometry (MS) and nuclear magnetic resonance (NMR) spectroscopy are superior over other analytical techniques such as Fourier transform infrared (FT-IR) spectroscopy (Corte et al., 2010; Ahmed et al., 2011; Rehman et al., 2012) and high-performance liquid chromatography (HPLC) method (Agnolet et al., 2012) due to high reproducibility of NMR-based techniques and high sensitivity or selectivity of MS-based techniques, and therefore are the most commonly used analytical tools in metabonomics/metabolomics research. NMR-based tools are in general used for nontargeted study and MS can be used for both selective and nonselective (targeted and nontargeted) analysis (Emwas et al., 2015). Although MS is thought to be more sensitive than NMR (Monteiro et al., 2013) and

* Corresponding authors.
E-mails: zhanglm@nxmu.edu.cn (L. Zhang), chenjing@nxmu.edu.cn (J. Chen).
[1] These authors contributed equally to this work.

https://doi.org/10.1016/j.bjp.2018.05.008

^{1}H NMR spectroscopy generates spectra with many overlapping signals which leads to uncertainties in the assignment and quantification of many metabolites (Emwas et al., 2015), NMR-based metabonomic analysis still has its own advantages of being relatively robust across many samples and fast (with spectra acquired within a few minutes) in addition to being a non-destructive process (Emwas et al., 2013). Its non-selectivity in detecting the metabolites and capacity of multiple metabolite quantification or minimal sample preparation demanded enables the detection of all soluble proton-containing small-molecular-weight metabolites that are present in concentrations above 10 μM providing both quantitative and structural information (Lei et al., 2008). Moreover, NMR techniques have no limit ion suppression effects as indicated in MS analysis (Scalbert et al., 2009).

In this study, therefore, NMR-based approach was performed to elucidate the toxicity mechanism of *S. alopecuroides* by hunting the altered toxic metabolites and biochemical pathways in rat plasma and urine after intragastrically administrated with 0.5 and 1 g/kg of *S. alopecuroides* each per day for successive 14 days. One more week as recovery period after stopping drug treatment was also designed to display if the toxicity effect of *S. alopecuroides* is reversible. This work will be beneficial to properly analyze and monitor its clinical safety in a system view.

Materials and methods

The wild seeds of *Sophora alopecuroides* L., Fabaceae, were harvested from the semi-desert area of Ningxia Hui Autonomous Region, China in July, 2015 (coordinates 38°47′N and 106°27′E) and identified by associate Prof. Jianjun Zhao (College of Pharmacy, Ningxia Medical University, China). A voucher specimen (SA-201507) has been deposited in the College of Pharmacy, Ningxia Medical University, for further references.

NaH_2PO_4, Na_2HPO_4, and sodium azide solutions were purchased from Yinchuan Wei Bo Xin Biological Co., Ltd. (Ningxia, China). D_2O and D_2O (TSP) were purchased from Qingdao Tenglong Weibo Technology Co., Ltd. (Shandong, China).

The dried seeds were grinded into the powders and extracted three times for 30 min each time with 65% ethanol (1:8, w/v) at an ambient temperature in an ultrasonic water bath (40 kHz). The filtered solutions were merged and concentrated to dryness on a rotary evaporation apparatus. The extract with yield of 25.1% (w/w, dried extract/crude herb) was redissolved by normal saline to strength of 1 g/ml and stored at 4 °C before use.

Thirty male Sprague-Dawley (SD) rats (180–220 g, 7 weeks old) were purchased from the Laboratory Animal Center of Ningxia Medical University (SCXK N, 2011-0001) and housed at a standard animal experimental laboratory, with a 12 h light/12 h dark cycle, a humidity of 40 ± 5%, and a constant temperature of 25 ± 1 °C. Animals were allowed free access to standard pellets and water for one week prior to the experiment. The experimental protocol was approved by the University Ethics Committee (Ningxia Medical University, China; ethic approval: 2015-013). All procedures involving animals were in accordance with the Regulations of the Experimental Animal Administration, State Committee of Science and Technology, People's Republic of China.

After one-week acclimatization, rats were randomly assigned to three groups (n = 10). *S. alopecuroides* treated groups were gavaged at dosage of 0.5 and 1 g/kg once per day for sequential 14 days. Control group was subjected to oral administration with normal saline only. The total experiment lasted 21 days, including 14 days of treatment with *S. alopecuroides* and 7 days of recovery time. Urine samples were collected at day −1 (before treatment), 7, 14 and day 21 with the addition of 50 μl sodium azide solutions (0.1%, w/w) to each tube, respectively. At day 14, five rats of each group were sacrificed to collect plasma for biochemical and NMR analysis. The remaining animals in each group were continued to feed until day 21. All the samples were stored at −80 °C before use.

Plasma biochemical analysis was performed by the Laboratory Biochemistry Assessments Center of Ningxia Medical University on an Olympus AU 400 automatic analyzer (Olympus optical Co., Ltd, Japan). Alanine aminotransferase (ALT), aspartate aminotransferase (AST), urea nitrogen (BUN), glucose (GLU), and creatinine (CREA) were assayed. Data were statistically analyzed using SPSS16.0 software with significance at $p < 0.05$ and 0.01.

The frozen urine samples were thawed, and a total 500 μl of urine sample was mixed with 100 μl of phosphate buffer (0.2 mol/l of Na_2HPO_4/NaH_2PO_4, pH 7.4) to minimize variations in the pH of the urine samples and then centrifuged (14,000 × g, 4 °C, 10 min) to remove any precipitates. The supernatant was transferred into 5 mm NMR tube. An aliquot of 100 μl of D_2O, containing 0.05% sodium 3-trimethylsilyl-(2,2,3,3-$^2H_4$)-1-propionate (TSP), was finally added. Plasma samples were thawed and centrifuged (14,000 × g, 4 °C, 10 min), then transferred into 5 mm NMR tubes, respectively. Also, 100 μl of D_2O was added into each tube.

^{1}H NMR spectra of urinary and plasma samples were collected at 298 Kona Bruker Avance 500 MHz spectrometer equipped with a Bruker inverse probe (Bruker Biospec, Erlangen, Germany). The NMR spectrum was recorded using the water-presaturated standard one-dimensional Carr-Purcell-Meiboom-Gill (CPMG) pulse sequence (recycle delay-9° (τ-180°-τ) n-acquisition), which eliminated the interference by macromolecules. The plasma and urine free induction decays (FID) were collected with 128 or 64 transient into 32 k data points using a spectral width of 10 kHz with a relaxation delay of 3 s, and relaxation time (2 nτ) of 100 ms. All the FID were multiplied by an exponential function with a line-broadening factor of 0.3 Hz before Fourier transformation.

All the spectra were manually phased and baseline corrected, bucketed and then automatically integrated with a self-developed automation routine in software MestreNova as recommended in the literature (Emwas et al., 2018). The chemical shifts were referenced to the methyl group of TSP at δ 0.00. Each spectrum was segmented into regions with a width of 0.04 ppm between δ 9.2 and δ 0.5 using MestReNova 2.0 (Mestre-lab Research SL). The δ 4.60–6.20 region in urine spectra and δ 4.70–5.20 region in serum spectra were excluded prior to statistical analysis to remove the variation in water suppression efficiency. All remaining regions of the spectra were then normalized to the total sum of the integrated spectral area to reduce any significant concentration differences (Holmes et al., 1994).

All ^{1}H NMR spectra were submitted to Principal Components Analysis (PCA) in the Simca-P$^+$11.0 software (Umetrics, Umeá, Sweden) for an unsupervised pattern recognition analysis to identify general metabolic trends and possible outliers. The orthogonal partial least squared discriminant analysis (OPLS-DA) algorithm at Pareto scaling approach was always used to find the main changing metabolites related to drug exposures (Liu et al., 2015). Subsequently, the distinguishable peak area of the selected metabolites from the NMR was extracted (normalized to the total spectra area) to further evaluate the time- and dose-dependence of S. alopecuroides related metabolite variations.

Results and discussion

As displayed in Table 1, aspartate aminotransferase (AST) was enhanced to 114.98 ± 5.75 and 123.8 ± 13.06 IU/l by SA-treatment at doses of 0.5 and 1 g/kg when compared with control (106.34 ± 4.18 IU/l). Also, both creatinine (CREA) and blood urea nitrogen (BUN) increased significantly. AST is the pivotal biochemical index of hepatic diseases. An increased AST might indicate

Table 1
Plasma chemical and biological parameters (mean ± SD, $n = 5$) at day 14.

Group	Dose (g/kg)	Parameters				
		GLU (mg/dl)	CREA (μmol/l)	AST (IU/l)	ALT (IU/l)	BUN (mmol/l)
Control	–	8.78 ± 1.32	41.62 ± 5.09	106.34 ± 4.18	44.32 ± 6.06	6.90 ± 0.27
SA	0.5	7.74 ± 1.35	50.24 ± 6.24[a]↑	114.98 ± 5.75[a]↑	46.66 ± 4.22	7.18 ± 0.18
	1.0	7.36 ± 0.85	56.52 ± 7.70[b]↑	123.8 ± 13.06[a]↑	49.12 ± 6.96	7.32 ± 0.29[a]↑

[a] Significance at $p < 0.05$ vs. control group.
[b] Significance at $p < 0.01$ vs. control group.
Abbreviations: CREA, creatinine; ALT, alanine aminotransferase; AST, aspartate aminotransferase; GLU, glucose; BUN, blood urea nitrogen.

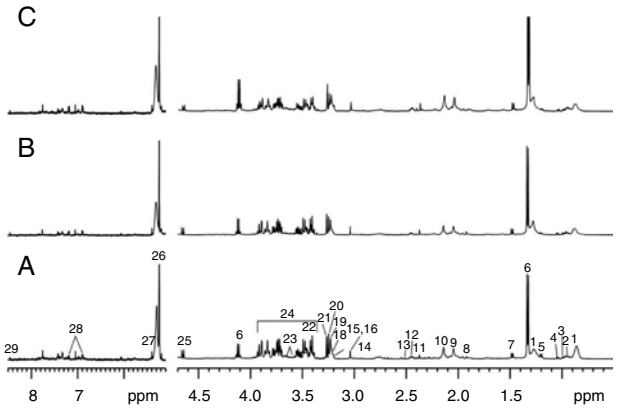

Fig. 1. Representative plasma 500 MHz ^{1}H NMR spectra of SD rats (A, control group; B, 0.5 g/kg of *Sophora alopecuroides*; C, 1.0 g/kg of *S. alopecuroides*). 1, lipids; 2, leucine; 3, isoleucine; 4, valine; 5, 3-hydroxy butyrate; 6, lactate; 7, alanine; 8, acetate; 9, N-acetyl glycoproteins; 10, O-acetyl glycoproteins; 11, pyruvate; 12, α-ketoglutarate; 13, dimethylamine; 14, dimethylglycine; 15, creatine; 16, creatinine; 17, choline 18, phosphorylcholine; 19, glycerol phosphorylcholine; 20, trimethylamine oxide/TMAO; 21, betaine; 22, taurine; 23, glycerol; 24, glucose and amino acids; 25, β-glucose; 26, α-glucose; 27, unsaturated lipids; 28, tyrosine; 29, formate.

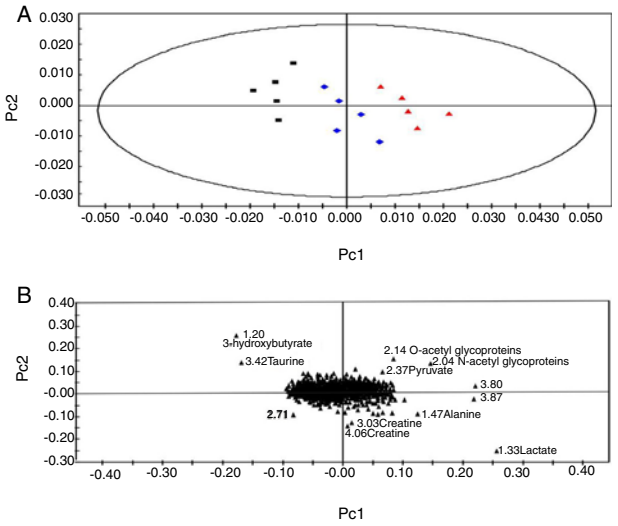

Fig. 2. Principal Component Analysis of plasma ^{1}H NMR spectra from control (■), rats treated with 0.5 g/kg of *Sophora alopecuroides* (♦) and rats treated with 1 g/kg of *S. alopecuroides* (▲) at day 14. (A) Scores plot; (B) loadings plot.

lesions or diseases in the liver induced by toxins (Liao et al., 2007). Blood urea nitrogen (BUN) is the product of amino acids and creatinine (CREA) is the ultimate product of creatine metabolism in skeletal muscle. Up-regulated BUN and CREA are important indicators of renal dysfunction (Sun et al., 2012). Therefore, it hinted that *S. alopecuroides* treatment might cause liver and kidney dysfunction of rats.

Representative plasma 500 MHz ^{1}H NMR spectra from the control and the groups treated with 0.5 and 1 g/kg of *S. alopecuroides* at day 14 were displayed in Fig. 1. Resonance and endogenous metabolites assignments were based on chemical shifts reported in the literatures (Li et al., 2008; Zhao et al., 2012). PCA method was applied to determine the extent of differences in the corresponding spectra between the *S. alopecuroides* treated and control groups. As shown in PCA score plots (Fig. 2A) and corresponding loading plots (Fig. 2B), the scores plot indicated that the metabolites of plasma in *S. alopecuroides* treatment groups is clearly distinct from those of the vehicle. Variations of the relative integrals from several metabolites were summarized in Table 2 accounting for the differentiation among three groups and listed the data from the statistical analysis. The identified major biochemical changes include increased lactate (δ 1.30, 4.14), pyruvate (δ 2.37), *N*-acetyl glycoproteins (δ 2.04), and alanine (δ 1.47) along with decreased 3-hydroxybutyrate (δ 1.20) and taurine (δ 3.26, 3.42).

Glycolysis is the preliminary and dominating process in glucose metabolism and exists in the cell cytoplasm where one glucose molecule is ultimately catalyzed to produce pyruvate by pyruvate kinase (PK). Pyruvate can be used to produce acetyl-CoA, which enters into tricarboxylic acid cycle (TCA cycle), playing a key role in glucose aerobic oxidation and energy production (Wu et al., 2008). In the ischemic or mitochondrial deficiency cells, pyruvate could be converted to lactate via lactate dehydrogenase (LDH) or to alanine via alanine amino transferase (ALT). In this paper, we observed that the disposal with 0.5 and 1 g SA/kg weight might lead to the glycolysis metabolism disorder and also an activated anaerobic metabolism based on explicitly increased biomarkers such as pyruvate and lactate in rat plasma.

3-HB is the ketone which is produced by lipids degradation through fatty acid oxidation. Mitochondria in the liver are the main sites for fatty acid oxidation, but the process of oxidation is always incomplete. Therefore, a part of the intermediate product named ketones including acetoacetate, 3-HB and acetone will produce. The peripheral tissue with the mitochondria oxidized 3-HB to acetoacetic acid and later to produce acetyl-CoA. And then the energy will be provided for the cells. Hence, down-regulated 3-HB in the plasma from SA-treated rats might suggest a damaged liver, insufficient oxidative capacity, weakened energy supply, and attenuated fatty acid metabolism.

Most of amino acids could be conversed to organic acids through the transamination effect catalyzed by alanine aminotransferase (ALT) and aspartate aminotransferase (AST) and later are decomposed to the substrates of TCA cycle. Alanine, as a non-essential amino acid, is highly concentrated in muscles and is one of the most important amino acids released by muscles. It will produce pyruvate through a reversible transamination effect and generate acetyl CoA into the TCA cycle (Guo et al., 2014). The up-regulated alanine level in the plasma from the SA-treated rats indicated an alanine metabolic pathway disorder.

Moreover, the aminotransferase is an intracellular enzyme. During the process of normal cell renewal, low concentrations of

Table 2
^{1}H NMR chemical shifts of the metabolites identified from the plasma and urine of rats treated with different doses of SA (mean ± SD, $n = 6$).

Samples	Metabolites	δ^1H (ppm)	Dose of SA-treatment (g/kg)	
			0.5	1.0
Plasma	Lipid	0.88 (t)	↓	↓
	3-Hydroxybutyrate	1.20 (d)	↓[a]	↓[a]
	Lactate	1.30 (d), 4.14 (q)	↑[a]	↑[a]
	N-acetyl glycoproteins	2.04 (s)	↑	↑[a]
	O-acetyl glycoproteins	2.14 (s)	↑	↑
	Alanine	1.47 (d)	↑[a]	↑[a]
	Taurine	3.26 (t), 3.42 (t)	↓[a]	↓[a]
	Pyruvate	2.37 (s)	↑[a]	↑[a]
	Creatine	3.04 (s), 3.94 (s)	↑	↑
	Glycerol	3.56 (dd)	↑	↑
Urine	Lactate	1.33 (d), 4.14 (q)	↓	↓
	Alanine	1.48 (d), 3.76 (q)	↓	↓
	Succinate	2.42 (s)	↓	↓[a]
	α-KG	2.45 (t), 3.02 (t)	↓[a]	↓[a]
	Citrate	2.54 (d), 2.70 (d)	↓	↓[a]
	Creatine	3.03 (s), 3.94 (s)	↓	↓
	Creatinine	3.06 (s), 4.06 (s)	↓	↓[a]
	Taurine	3.26 (t), 3.42 (t)	↑[a]	↑[a]
	TMAO	3.27 (s), 3.90 (s)	↑[a]	↑[a]
	Glycine	3.57 (s)	↓	↓
	Phenylalanine	7.42 (m)	↑	↑
	Hippurate	7.56 (m), 7.62 (m), 7.83 (m)	↑[a]	↑[a]

Multiplicity: s, single; d, double; t, triplet; q, quartet; m, multiplet.
[a] Significance at $p < 0.05$ vs. control group.
Abbreviations: α-KG, α-ketoglutarate; TMAO, trimethylamine oxide.

aminotransferase always occur in the plasma. Therefore, elevated aminotransferase concentrations suggest cell damage. The appearance of AST and ALT in the plasma has a special diagnostic value. Almost all liver diseases could lead to an elevated level of AST and ALT in the plasma which might result in an extensive liver cell necrosis (Waterfield et al., 1993; Clayton et al., 2003). Our data (Table 1) demonstrated that *S. alopecuroides* treatment impaired the liver based on an enhanced AST and ALT in contrast with the vehicle.

We observed a decreased tendency for a key biomarker, taurine, in the plasma from SA-treated rats. Taurine is one of the most abundant free amino acids presented in mammalian tissues with various biological functions (Brown et al., 1993), such as stabilizing cell membranes, scavenging oxygen free radicals, regulating intracellular osmostasis, and maintaining an intracellular Ca^{2+} concentration (Wang et al., 1996; Condron et al., 2003; Maher et al., 2005). Taurine, therefore, has a hepatoprotective effect against oxidative stress such as lipid peroxidation. Hence, a declined level of taurine indicated an over-consumption to counteract the injury of oxidative stress induced by SA treatment.

The typical 500 MHz ^{1}H NMR spectra of urine samples were also obtained from the control and SA-treated rats (Fig. 3). Endogenous metabolites involved in ^{1}H NMR chemical shift assignments were assigned according to the literatures (Solanky et al., 2003; Coen et al., 2003; Garrod et al., 2005; Ding et al., 2009; Hwang et al., 2009; Zhang et al., 2011; Tang et al., 2004; Li et al., 2015; Wang et al., 2018). From PCA-derived scores plot, the separation of *S. alopecuroides* treated groups from the control is evident (Fig. 4A). A loadings plot (Fig. 4B) is generated to identify the metabolites responsible for the differentiation in the scores plot. It shows increased levels of taurine (δ 3.26, 3.42), TMAO (δ 3.27, 3.90) and hippurate (δ 7.56, 7.62, and 7.83) along with decreased levels of succinate (δ 2.42), α-KG (δ 2.45, 3.02), citrate (δ 2.54, 2.70), and creatinine (δ 3.06, 4.06) in *S. alopecuroides* treated groups when compared with control group. The ^{1}H NMR-detected relative integral level of variation metabolites in urine samples of different groups was also summarized in Table 2.

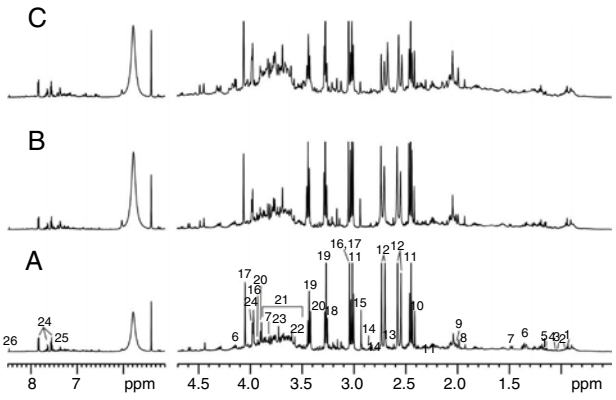

Fig. 3. Representative urine 500 MHz ^{1}H NMR spectra of SD rats (A – Control group; B – 0.5 g/kg of *Sophora alopecuroides*; C – 1 g/kg of *S. alopecuroides*). 1, leucine; 2, isoleucine; 3, valine; 4, 3-methy-2-ketovalerate; 5, 2-ketovalerate; 6, lactate; 7, alanine; 8, acetate; 9, N-acetyl glycoproteins; 10, succinate; 11, α-ketoglutarate; 12, citrate; 13, methylamine; 14, trimethylamine; 15, dimethyl glycine; 16, creatine; 17, creatinine; 18, TMAO; 19, betaine; 20, taurine; 21, glucose; 22, glycine; 23, glutamine; 24, hippurate; 25, phenylalanine; 26, formate.

Acetylcholine (ACh) is the principal neurotransmitter in the parasympathetic nerve. The release of ACh is always accompanied by a variety of physiological activities. It will be hydrolyzed into choline and acetic acid right after releasing under the hydrolysis effect by cholinesterase. The final production of creatine and creatinine by oxidation is the dominating metabolic pathway of choline. In this paper, a decreased level of creatinine in the urine in SA-treated rats suggested that the SA-toxicity caused an information transmission disorder. Creatinine is a waste product formed by a slow spontaneous degradation of creatine-phosphate (Wyss and Kaddurah-Daouk, 2000). Creatine-phosphate functions as an energy conditioner that stores the energy of excess ATP (Ma et al., 2010a,b). As reported (Bell et al., 1991; Zhang et al., 2012), urinary creatinine might be considered as a biomarker of renal function.

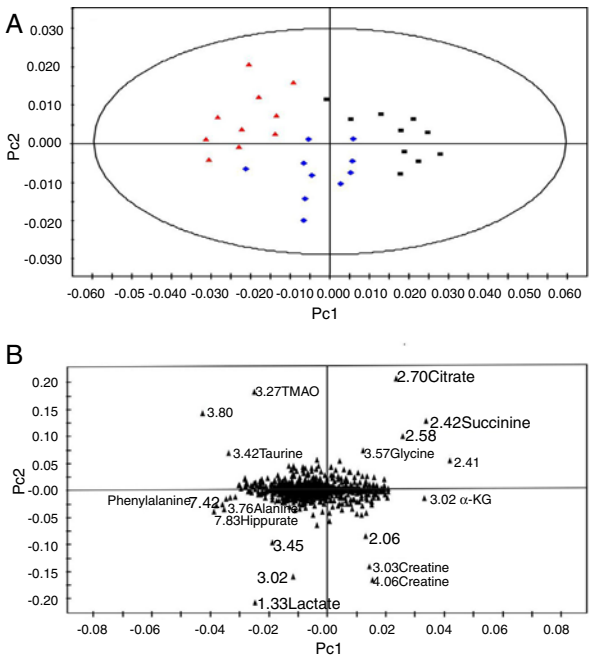

Fig. 4. Principal component analysis of urine ^{1}H NMR spectra from control (■), rats treated with 0.5 g/kg of *Sophora alopecuroides* (♦) and rats treated with 1 g/kg of *S. alopecuroides* (▲) at day 14. (A) Scores plot; (B) loadings plot.

Choline can still be decomposed to be methylamine metabolites such as DMA, TMA, and TMAO by gut microbiota (Gullans et al., 1988; Gartland et al., 1989; Foxall et al., 1993; Holmes et al., 1995, 1997; Feng et al., 2002). An up-regulated TMAO level in the urine in *S. alopecuroides* treated rats indicated that the gut microbiota had a high speed in choline metabolism under the pressure of *S. alopecuroides*. The metabolic activity of gut microbiota increased the choline metabolism in SA-treated rats, and produced much more methylamine metabolites. The toxicity of *S. alopecuroides*, therefore, makes a dynamic imbalance of intestinal flora for the rats.

We also found that the biomarker hippurate in the urine was enhanced in *S. alopecuroides* treated rats. The production of hippuric acid requires the formation of benzoic acid by the decomposition of the phenyl group with the gut microbiota (Phipps et al., 1998; Williams et al., 2002; Nicholls et al., 2003), and then is combined with glycine in the liver under the action of cytochrome. It again demonstrated that *S. alopecuroides* actually induced a gut microbiota disorder.

Finally, the same PCA strategy was applied to the urinary metabonomic study after *S. alopecuroides* treatment at doses of 0.5 g and 1 g/kg at four matched time points (days −1, 7, 14, and 21) to reveal the time-related response to SA treatment (Fig. 5). The loading plots indicated the corresponding changes in metabolites during treatment duration and recovery for both two SA treatment groups, such as increased TMAO and taurine as well as decreased succinate and α-KG. The normalized integrals of the changes in these endogenous urinary metabolites were shown in Fig. 5, which demonstrated the time-related response to *S. alopecuroides* treatment. It comes to reach a conclusion that the toxicity effect of *S. alopecuroides* might be irreversible.

PCA analysis of ^{1}H NMR metabonomic profiles of plasma and urine samples revealed the potential toxic biomarkers and the altered metabolic pathways induced by *S. alopecuroides* caused toxicity. The corresponding metabolic pathways included TCA cycle, anaerobic glycolysis, amino acid metabolism, and gut microbe disorder (Fig. 6).

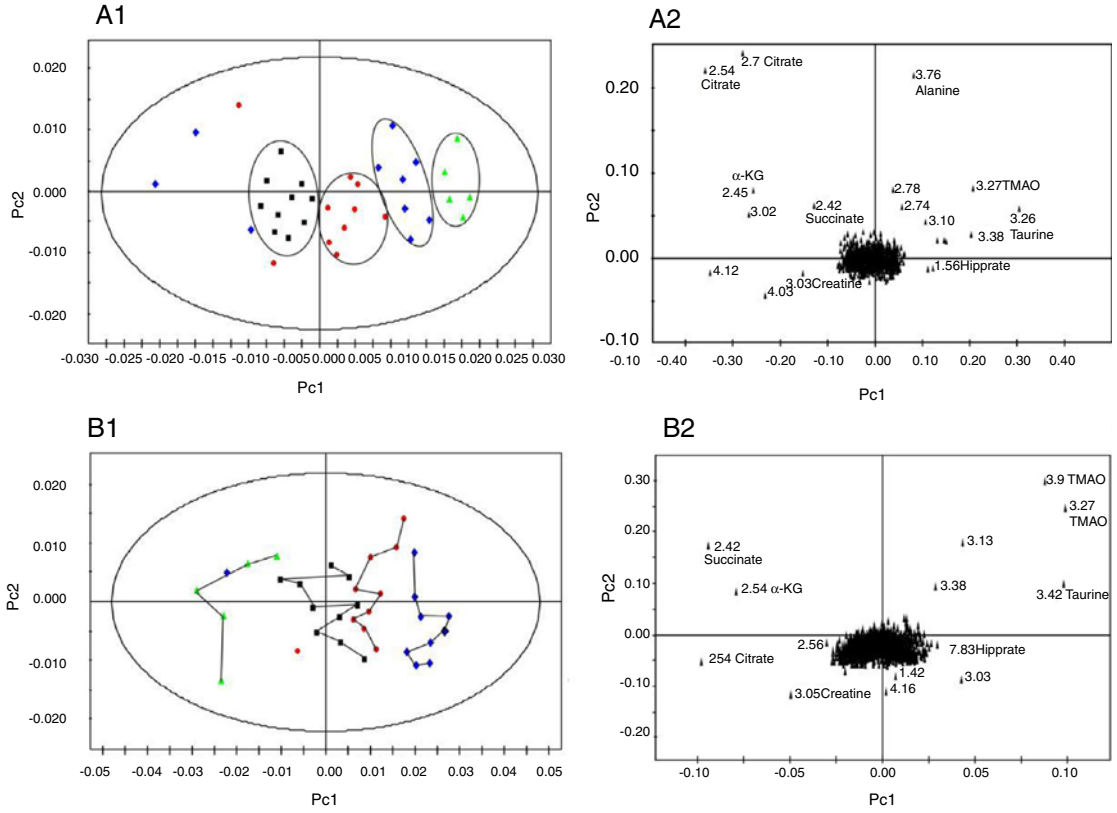

Fig. 5. Principal component analysis of urine ^{1}H NMR spectra of SD rats treated with 0.5 g/kg of *Sophora alopecuroides* (A1 and A2, R2 = 86.3%, Q2 = 74.80%) and 1 g/kg of *S. alopecuroides* at four matched time points (day −1 (■), 7 (●), 14 (♦), and 21 (▲)).

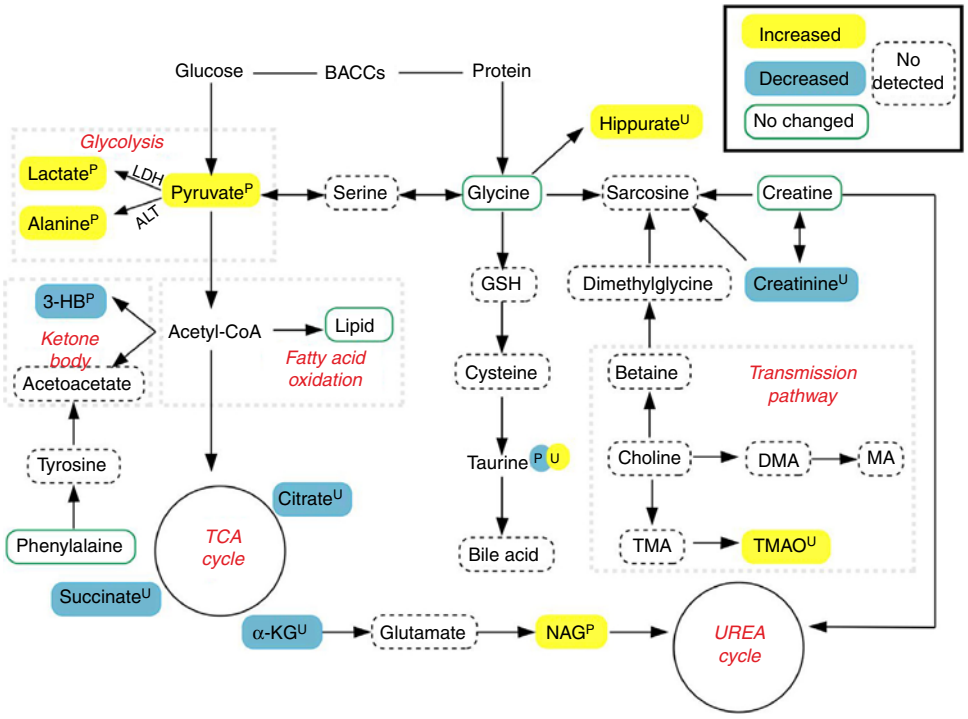

Fig. 6. Schematic diagram of the disturbed metabolic pathways were detected by ^{1}H NMR analysis, showing the interrelationship of the identified metabolic pathways. The words in yellow means increased biomarkers and words in blue means decreased biomarkers. Metabolites with superscript "P" means observed significant level change from plasma; "U" means observed significant level change from urine; "PU" means observed significant level change from both plasma and urine.

Conclusion

In this study, ^{1}H NMR based metabonomic analysis using plasma and urine samples in conjunction with plasma biochemistry assay was performed to investigate the toxic metabolites biomarkers and abnormal biochemical pathways caused by toxicity of *S. alopecuroides*. Dose- and time-related changes of endogenous metabolites in *S. alopecuroides* treated rats included increased lactate, alanine, *N*-acetyl glycoproteins, creatine, alanine, and pyruvate along with decreased 3-hydroxybutyrate and taurine in plasma samples. Increased taurine, TMAO, and hippurate as well as decreased succinate, α-KG, citrate, and creatinine in urine samples were also discovered. Altered biochemical pathways included energy metabolism, amino acid metabolism and gut microbiota. Toxicity of SA, therefore, is evaluated through a systematic and holistic view.

Author's contributions

JC and CZ contributed in running the laboratory work. XW and HJ analyzed the data. WM and SW revised the manuscript critically. LZ and JC designed the study, supervised the laboratory work and contributed to modify the manuscript. All the authors have read the final manuscript and approved its submission.

Ethical disclosures

Protection of human and animal subjects. The authors declare that the procedures followed were in accordance with the regulations of the relevant clinical research ethics committee and with those of the Code of Ethics of the World Medical Association (Declaration of Helsinki).

Confidentiality of data. The authors declare that they have followed the protocols of their work center on the publication of patient data.

Right to privacy and informed consent. The authors declare that no patient data appear in this article.

Conflicts of interest

The authors declare no conflicts of interest.

Acknowledgement

This work was supported by Ningxia Natural Science Foundation (NZ17056).

References

Ahmed, A.E.S.I., Wardell, J.N., Thumser, A.E., Avignone-Rossa, C.A., Cavalli, G., Hay, J.N., Bushell, M.E., 2011. Metabolomic profiling can differentiate between bactericidal effects of free and polymer bound halogen. J. Appl. Polym. Sci. 119, 709–718.

Agnolet, S., Wiese, S., Verpoorte, R., Staerk, D., 2012. Comprehensive analysis of commercial willow bark extracts by new technology platform: combined use of metabolomics, high-performance liquid chromatography-solid-phase extraction-nuclear magnetic resonance spectroscopy and high-resolution radical scavenging assay. J. Chromatogr. A 1262, 130–137.

Bell, J.D., Sadler, P.J., Morris, V.C., Levander, O.A., 1991. Effect of aging and diet on proton NMR spectra of rat urine. Magn. Reson. Med. 17, 414–422.

Boudonck, K.J., Mitchell, M.W., Német, L., Keresztes, L., Nyska, A., Shinar, D., Rosentock, M., 2009a. Discovery of metabolomics biomarkers for early detection of nephrotoxicity. Toxicol. Pathol. 37, 280–292.

Boudonck, K.J., Rose, D.J., Karoly, E.D., Lee, D.P., Lawton, K.A., Lapinskas, P.J., 2009b. Metabolomics for early detection of drug-induced kidney injury: review of the current status. Bioanalysis 9, 1645–1663.

Brown, D.A., Higashida, H., Noda, M., Ishizaka, N., Hashii, M., Hoshi, N., Yokoyama, S., Fukuda, K., Katayama, M., Nukada, T., 1993. Coupling of muscarinic receptor subtypes to ion channels: experiments on neuroblastoma hybrid cells. Ann. N.Y. Acad. Sci. 707, 237–258.

Cai, Y.M., Gao, Y., Tan, G.G., Wu, S., Dong, X., Lou, Z.Y., Zhu, Z.Y., Chai, Y.F., 2013. Myocardial lipidomics profiling delineate the toxicity of traditional Chinese medicine *Aconiti lateralis* radix praeparata. J. Ethnopharmacol. 147, 349–356.

Clayton, T.A., Lindon, J.C., Everet, J.R., Charuel, C., Hanton, G., Le Net, J.L., Provost, J.P., Nicholson, J.K., 2003. An hypothesis for a mechanism underlying hepatotoxin-induced hypercreatinuria. Arch. Toxicol. 77, 208–217.

Coen, M., Lenz, E.M., Nicholson, J.K., Wilson, I.D., Pognan, F., Lindon, J.C., 2003. An integrated metabonomic investigation of acetaminophen toxicity in the mouse using NMR spectroscopy. Chem. Res. Toxicol. 16, 295–303.
Condron, C., Neary, P., Toomey, D., Redmond, H.P., Bouchier-Hayes, D., 2003. Taurine attenuates calcium-dependent, Fas-mediated neutrophil apoptosis. Shock 19, 564–569.
Corte, L., Rellini, P., Roscini, L., Fatichenti, F., Cardinali, G., 2010. Development of a novel, FTIR (Fourier transform infrared spectroscopy) based, yeast bioassay for toxicity testing and stress response study. Anal. Chim. Acta 659, 258–265.
Ding, L., Hao, F., Shi, Z.M., Wang, Y.L., Zhang, H.X., Tang, H.R., Dai, J.Y., 2009. Systems biological responses to chronic perfluorododecanoic acid exposure by integrated metabonomic and transcriptomic studies. J. Proteome Res. 8, 2882–2891.
Emwas, A.H.M., Salek, R.M., Griffin, J.L., Merzaban, J., 2013. NMR-based metabolomics in human disease diagnosis: applications, limitations, and recommendations. Metabolomics 9, 1048–1072.
Emwas, A.H., Luchinat, C., Turano, P., Tenori, L., Roy, R., Salek, R.M., Ryan, D., Merzaban, J.S., Kaddurah-Daouk, R., Zeri, A.C., Gowda, G.A.N., Raftery, D., Wang, Y.L., Brennan, L., Wishart, D.S., 2015. Standardizing the experimental conditions for using urine in NMR-based metabolomic studies with a particular focus on diagnostic studies: a review. Metabolomics 11, 872–894.
Emwas, A.H.M., Saccenti, E., Gao, X., Mckay, R.T., Dos Santos, V.A.P.M., Roy, R., Wishart, D.S., 2018. Recommended strategies for spectral processing and post-processing of 1D ^{1}H-NMR data of biofluids with a particular focus on urine. Metabolomics 14, 31–54.
Feng, J., Li, X., Pei, F., Chen, X., Li, S., Nie, Y., 2002. ^{1}H NMR analysis for metabolites in serum and urine from rats administrated chronically with La (NO). Anal. Biochem. 301, 1–7.
Foxall, P.J.D., Mellotte, G.J., Bending, M.R., Lindon, J.C., Nicholson, J.K., 1993. NMR spectroscopy as a novel approach to the monitoring of renal transplant function. Kidney Int. 43, 234–245.
Garrod, S., Bollard, M.E., Nicholls, A.W., Connor, S.C., Connelly, J., Nicholson, J.K., Holmes, E., 2005. Integrated metabonomic analysis of the multi organ effects of hydrazine toxicity in the rat. Chem. Res. Toxicol. 18, 115–122.
Gartland, K.P., Bonner, F.W., Nicholson, J.K., 1989. Investigations into the biochemical effects of region-specific nephrotoxins. Mol. Pharmacol. 35, 242–250.
Gullans, S.R., Blumenfeld, J.D., Balschi, J.A., Kaleta, M., Brenner, R.M., Heilig, C.W., Herbert, S.C., 1988. Accumulation of major organic osmolytes in rat renal inner medulla in dehydration. AJP: Renal. Physiol. 241, 626–634.
Guo, P.P., Wang, J.S., Dong, G., Wei, D.D., Li, M.H., Yang, M.H., Kong, L.Y., 2014. NMR-based metabolomics approach to study the chronic toxicity of crude ricin from castor bean kernels on rats. Mol. Biosyst. 10, 2426–2440.
Holmes, E., Bonner, F.W., Nicholson, J.K., 1997. ^{1}H NMR spectroscopic and histopathological studies on propyleneimine-induced renal papillary necrosis in the rat and multimammate desert mouse (*Mastomys natalensis*). Comp. Biochem. Physiol. C: Pharmacol. Toxicol. Endocrinol. 116, 125–134.
Holmes, E., Caddick, S., Lindon, J.C., Wilson, I.D., Kryvawych, S., Nicholson, J.K., 1995. ^{1}H and ^{2}H NMR spectroscopic studies on the metabolism and biochemical effects of 2-bromoethanamine in the rat. Biochem. Pharmacol. 49, 1349–1359.
Holmes, E., Foxall, P.J., Nicholson, J.K., Neild, G.H., Brown, S.M., Beddell, C.R., Sweatman, B.C., Rahr, E., Lindon, J.C., Spraul, M., 1994. Automatic data reduction and pattern recognition methods for analysis of ^{1}H nuclear magnetic resonance spectra of human urine from normal and pathological states. Anal. Biochem. 220, 284–296.
Hwang, G.S., Yang, J.Y., Ryu, D.H., Kwon, T.H., 2009. Metabolic profiling of kidney and urine in rats with lithium-induced nephrogenic diabetes insipidus by ^{1}H-NMR-based metabonomics. Am. J Physiol. Renal. 298, 461–470.
Ji, J., Zhang, L.J., Zhang, H.X., Sun, C., Sun, J.D., Jiang, H., Abdalhai, M.H., Zhang, Y.Z., Sun, X.L., 2016. ^{1}H NMR-based urine metabolomics for the evaluation of kidney injury in Wistar rats by 3-MCPD. Toxicol. Res. 5, 689–696.
Lei, R.H., Wu, C.Q., Yang, B.H., Ma, H.Z., Shi, C., Wang, Q., Wang, Q.J., Yuan, Y., Liao, M.Y., 2008. Integrated metabolomic analysis of the nano-sized copper particle-induced hepatotoxicity and nephrotoxicity in rats: a rapid in vivo screening method for nanotoxicity. Toxicol. Appl. Pharm. 232, 292–301.
Li, L., Sun, B., Zhang, Q., Fang, J.J., Ma, K.P., Li, Y., Chen, H.B., Dong, F.T., Gao, Y., Li, F.M., Yan, X.Z., 2008. Metabonomic study on the toxicity of Hei-Shun-Pian, the processed lateral root of *Aconitum carmichaelii* Debx (Ranunculaceae). J. Ethnopharmacol. 116, 561–568.
Li, D., Zhang, L.L., Dong, F.C., Liu, Y., Li, N., Li, H.H., Lei, H.H., Wang, Y.L., Zhu, Y., Tang, H.R., 2015. Metabonomic changes associated with atherosclerosis progression for LDLR$^{-/-}$ mice. J. Proteome Res. 14, 2237–2254.
Liao, P.Q., Wei, L., Zhang, X.Y., Li, X.J., Wu, H.F., Wu, Y.J., Ni, J.Z., Pei, F.K., 2007. Metabolic profiling of serum from gadolinium chloride-treated rats by ^{1}H NMR spectroscopy. Anal. Biochem. 364, 112–121.
Liu, C.C., Wu, Y.F., Feng, G.M., Gao, X.X., Zhou, Y.Z., Hou, W.J., Qin, X.M., Du, G.H., Tian, J.S., 2015. Plasma-metabolite-biomarkers for the therapeutic response in depressed patients by the traditional Chinese medicine formula Xiaoyaosan: a ^{1}H NMR-based metabolomics approach. J. Affect. Disord. 185, 156–163.
Ma, C., Bi, K.S., Zhang, M., Su, D., Fan, X.X., Ji, W., Wang, C., Chen, X.H., 2010a. Metabonomic study of biochemical changes in the urine of morning glory seed treated rat. J. Pharm. Biomed. Anal. 53, 559–566.
Ma, C., Bi, K.S., Zhang, M., Su, D., Fan, X.X., Ji, W., Wang, C., Chen, X.H., 2010b. Toxicology effects of morning glory seed in rat: a metabonomic method for profiling of urine metabolic changes. J. Ethnopharmacol. 130, 134–142.
Maher, S.G., Condron, C.E.M., Bouchier-Hayes, D.J., Toomey, D.M., 2005. Taurine attenuates CD3/interleukin-2-induced T cell apoptosis in an in vitro model of activation-induced cell death (AICD). Clin. Exp. Immunol. 139, 279–286.
Monteiro, M.S., Carvalho, M., Bastos, M.L., Guedes de Pinho, P., 2013. Metabolomics analysis for biomarker discovery: advances and challenges. Curr. Med. Chem. 20, 257–271.
Nicholls, A.W., Mortishire-Smith, R.J., Nicholson, J.K., 2003. NMR spectroscopic based metabonomic studies of urinary metabolite variation in acclimatizing germ-free rats. Chem. Res. Toxicol. 16, 1395–1404.
Phipps, A.N., Stewart, J., Wright, B., Wilson, I.D., 1998. Effect of diet on the urinary excretion of hippuric acid and other dietary derived aromatics in rat. A complex interaction between diet, gut microflora and substrate specificity. Xenobiotica 28, 527–537.
Rehman, S., Xu, Y., Dunn, W.B., Day, P.J.R., Westerhoff, H.V., Goodacre, R., Bayat, A., 2012. Dupuytren's disease metabolite analyses reveals alterations following initial short-term fibroblast culturing. Mol. Bio Syst. 8, 2274–2288.
Ren, D., 2000. Development and clinical application of compounded *Sophora alopecuroides* oral ulcer composite film. Chinese Traditional Patent Medicine 8, 62–63.
Scalbert, A., Brennan, L., Fiehn, O., Hankemeier, T., Kristal, B.S., Ommen, B., Pujos-Guillot, E., Verheij, E., Wishart, D., Wopereis, S., 2009. Mass-spectrometry-based metabolomics: limitations and recommendations for future progress with particular focus on nutrition research. Metabolomics 5, 435–458.
Solanky, K.S., Bailey, N.J., Beckwith-Hall, B.M., Davis, A., Bingham, S., Holmes, E., Nicholson, J.K., Cassidy, A., 2003. Application of biofluid ^{1}H nuclear magnetic resonance-based metabonomic techniques for the analysis of the biochemical effects of dietary isoflavones on human plasma profile. Anal. Biochem. 323, 197–204.
Sun, Y.J., Wang, H.P., Liang, Y.J., Yang, L., Li, W., Wu, Y.J., 2012. An NMR-based metabonomic investigation of the subacute effects of melamine in rats. J. Proteome Res. 11, 2544–2550.
Tang, H., Wang, Y., Nicholson, J.K., Lindon, J.C., 2004. Use of relaxation-editedone-dimensional and two dimensional nuclear magnetic resonance spectroscopy to improve detection of small metabolites in blood plasma. Anal. Biochem. 325, 260–272.
Wang, J.H., Redmond, H.P., Watson, R.W., Condron, C., Bouchier-Hayes, D., 1996. The beneficial effect of taurine on the prevention of human endothelial cell death. Shock 6, 331–338.
Wang, X.R., Wang, D.Z., Zhou, Z.Q., Zhu, W.T., 2018. Subacute oral toxicity assessment of benalaxyl in mice based on metabolomics methods. Chemosphere 191, 373–380.
Waterfield, C.J., Turton, J.A., Scale, M.D.C., Timbrell, J.A., 1993. Investigations into the effects of various hepatotoxic compounds on urinary and liver taurine levels in rats. Arch. Toxicol. 67, 244–254.
Williams, R.E., Eyton-Jones, H.W., Farnworth, M.J., Gallagher, R., Provan, W.M., 2002. Effect of intestinal microflora on the urinary metabolic profile of rats: a ^{1}H-nuclear magnetic resonance spectroscopy study. Xenobiotica 32, 783–794.
Wu, B., Yan, S.K., Lin, Z.Y., Wang, Q., Yang, Y., Yang, G.J., Shen, Z.Y., Zhang, W.D., 2008. Metabonomic study on ageing: NMR-based investigation into rat urinary metabolites and the effect of the total flavone of epimedium. Mol. Bio Syst. 4, 855–861.
Wu, C., Chen, C.H., Chen, H.C., Liang, H.J., Chen, S.T., Lin, W.Y., Wu, K.Y., Chiang, S.Y., Lin, C.Y., 2017. Nuclear magnetic resonance- and mass spectrometry-based metabolomics to study maleic acid toxicity from repeated dose exposure in rats. J. Appl. Toxicol. 37, 1493–1506.
Wyss, M., Kaddurah-Daouk, R., 2000. Creatine and creatinine metabolism. Physiol. Rev. 80, 1107–1213.
Xiao, P.G., 1993. A Pictorial Encyclopedia of Chinese Medical Herbs, Japanese Edition. Chuokoron-Sha Inc, Tokyo, pp. 110.
Yang, J.X., Yu, Z.F., 1998. Research progress of *Sophora alopecuroides* L. Tianjin Pharmacy 10, 43–45.
Yin, J.B., Liu, S., Yu, J., Wu, B., 2017. Differential toxicity of arsenic on renal oxidative damage and urinary metabolic profiles in normal and diabetic mice. Environ. Sci. Pollut. Res. Int. 24, 17485–17492.
Zhang, H.X., Ding, L.N., Fang, X.M., Shi, Z.M., Zhang, Y.T., Chen, H.B., Yan, X.Z., Dai, J.Y., 2011. Biological responses to perfluorododecanoic acid exposure in rat kidneys as determined by integrated proteomic and metabonomic studies. PLoS ONE 6, e20862.
Zhang, Y.W., Yan, S.K., Gao, X., Xiong, X.S., Dai, W.X., Liu, X.R., Li, L., Zhang, W.D., Mei, C.L., 2012. Analysis of urinary metabolic profile in aging rats undergoing caloric restriction. Aging Clin. Exp. Res. 24, 79–84.
Zhang, Z.H., Zhao, Y.Y., Cheng, X.L., Dai, Z., Zhou, C., Bai, X., Lin, R.C., 2013. General toxicity of *Pinellia ternata* (Thunb.) Berit. in rat: a metabonomic method for profiling of serum metabolic changes. J. Ethnopharmacol. 149, 303–310.
Zhao, L.C., Gao, H.C., Zhao, Y.X., Lin, D.H., 2012. Metabonomic analysis of the therapeutic effect of Zhibai Dihuang Pill in treatment of streptozotocin-induced diabetic nephropathy. J. Ethnopharmacol. 142, 647–656.